Effect of cobalt content on the properties of quintuple perovskites $Sm_2Ba_3Fe_5$-xCo_xO_{15}-δ

EFFECT OF COBALT CONTENT ON THE PROPERTIES OF QUINTUPLE PEROVSKITES $Sm_2Ba_3Fe_{5-x}Co_xO_{15-\delta}$

I.B. Golovachev[a], M.Yu. Mychinko[b], N.E. Volkova[a*], L.Ya. Gavrilova[a], B. Raveau[c], A. Maignan[a,c], V.A. Cherepanov[a]

[a] *Institute of Natural Science and Mathematics, Ural Federal University, Lenin av., 51, Yekaterinburg, 620000, Russia*

[b] *Electron Microscopy for Materials Science (EMAT), University of Antwerp, Groenenborgerlaan 171, 2020 Antwerp, Belgium*

[c] *Laboratoire CRISMAT, UMR 6508 Normandie Université, CNRS, ENSICAEN, UNICAEN, 6 bd du Maréchal Juin, 14050 CAEN Cedex 4, France*

* - corresponding author: nadezhda.volkova@urfu.ru

Abstract:

Quintuple perovskites $Sm_2Ba_3Fe_{5-x}Co_xO_{15-\delta}$ (x = 0.5, 1.0 and 1.5) have been prepared by glycerin-nitrate technique in air. The phase purity was confirmed by XRD. Partial substitution of Co for Fe decreases oxygen content and thus the mean oxidation state of 3*d*-metals. It also slightly decreases thermal expansion coefficient of oxides. Positive value of Seebeck coefficient confirmed *p*-type conductivity, though the thermopower decreases as the Co content increases. Temperature dependence of electrical conductivity reveals a maximum at 550-750°C.

Keywords

Multilayer structure, Semiconductors, Electrical properties, Thermal properties

1. Introduction:

Layered perovskites are considered as promising cathode materials for intermediate-temperature solid oxide fuel cell (IT-SOFC) because of their superior mixed electronic–ionic conduction properties and high thermal stability [1-11].

Recently a new class of 5-fold layered nanoscale-ordered $Ln_{2-\varepsilon}Ba_{3+\varepsilon}Fe_5O_{15-\delta}$ oxides was detected in the $Ln_2O_3 - BaO - Fe_2O_3$ (Ln= Nd, Sm, Eu, Gd) systems in air [12-16]. This 5-fold layered structure is formed by alternation of the layers containing exclusively lanthanide or barium together with the mixed (Ln,Ba) layers along the c-axis in a sequence: Ln-Ba-(Ln,Ba)-(Ln,Ba)-Ba-Ln. The oxygen content, which is closely related with oxidation state of 3*d* metals, plays an important role in formation of quintuple perovskite superstructure. In Co-free samarium barium ferrite the required oxygen content in air condition can be achieved only by means of partial substitution (ε) of Ba for Sm forming $Ln_{2-\varepsilon}Ba_{3+\varepsilon}Fe_5O_{15-\delta}$ with ε=0.125. Here barium serves as an acceptor-type dopant Ba'_{Sm} located in a mixed (Ln/Ba) layer and thus allow decreasing the value of oxygen content (raise oxygen vacancy concentration $[V_O^{\cdot\cdot}]$). Partial substitution of Co for Fe makes unnecessary stoichiometry deviation in A-site sublattice (ε=0) since in this case cobalt ions serve as acceptor-type substituent Co'_{Fe} and allow decreasing oxygen content in $Sm_2Ba_3Fe_{5-x}Co_xO_{15-\delta}$ down to its favorable value [13-16].

The aforementioned complex layered structure was also attracting attention in terms of practical application. Co-free quintuple perovskite

$Sm_{1.875}Ba_{3.125}Fe_5O_{15-\delta}$ was recently considered as a novel cathode for IT-SOFCs [17].

Since both oxygen content and substitution of Co for Fe govern the formation of 5-fold layered superstructure, in this paper we examined the effect of Co introduction on oxygen content, electrical properties and thermal expansion of $Sm_2Ba_3Fe_{5-x}Co_xO_{15-\delta}$ (x = 0.5–1.5) solid solutions.

2. Material and methods:

The samples of $Sm_2Ba_3Fe_{5-x}Co_xO_{15-\delta}$ (x = 0.5, 1.0 and 1.5) were prepared using a glycerin nitrate technique using high-purity Sm_2O_3, $BaCO_3$, $FeC_2O_4\times2H_2O$, Co, HNO_3 and glycerol as starting materials. The starting reagents weighted in the required amounts were dissolved in nitric acid, and then glycerol was added to the solution. Further details of glycerol-nitrate technique were described earlier elsewhere [16]. Final anneals were performed at 1100ºC in air during for 120 h employing several steps (≈20 h each) and intermediate grinding. Finally, samples were slowly cooled to room temperature at a rate of about 70°C/h. The phase composition of the annealed samples was determined by X-ray diffraction (XRD) using a Shimadzu XRD-7000 instrument (CuKα-radiation, angle range 2Θ= 20°–90°, step 0.02°, 5 s/step) in air. The structural parameters were refined by the Le-Bail method using the Fullprof-2008 package. Thermogravimetric analysis (TGA) was carried out using a STA 409PC instrument (Netzsch) within the temperature range 25–1100°C in air in dynamic (heating/cooling rate 5°C/min) mode and static mode (isothermal exposure for 8 h). Thermal expansion of ceramic samples was measured using a high temperature dilatometer DIL 402 C (Netzsch) in the temperature range 25–1100°C in air with the heating/cooling rate of 5°C/min. Total electrical conductivity (σ) and the Seebeck coefficient (S) of ceramic samples were measured by a standard 4-probe DC method with platinum electrodes within the

temperature range 25–1100°C. Temperature control and data collection were performed with a Zirconia 318 instrument [18]. Dense ceramic samples in the form of bars (3×3×25 mm^3) for dilatometry and electrical properties measurements were prepared by uniaxial pressing of the powders under pressure of 20 bar, followed by sintering at 1300-1350°C for 12 h. The samples were slowly cooled to room temperature at a rate of 50 °C/h. The densities of the polished ceramic samples were 92–95% of the theoretical value calculated from the XRD data.

3. Results and discussion:

It was shown already by HRTEM that all $Sm_2Ba_3Fe_{5-x}Co_xO_{15-\delta}$ (x=0.5-1.5) oxides possess 5-fold tetragonal $a_p \times a_p \times 5a_p$ superstructure [16]. Although XRD analysis cannot detect the formation of layered ordered supercell due to the chemical twinning along the orthogonal directions [12-16] it can confirm single phase purity. Accordingly, the XRD results of all obtained samples were single-phase that can be described in terms of the cubic perovskite structure (SG $Pm\bar{3}m$). The XRD patterns for the single-phase $Sm_2Ba_3Fe_{5-x}Co_xO_{15-\delta}$ refined by the Le-Bail method are presented in supplementary (Fig. S1). The refined unit cell parameters were found to be in good agreement with those reported in ref. [16]. No traces of starting materials or secondary phase were detected.

Fig. 1 illustrates the variations of oxygen content in $Sm_2Ba_3Fe_{5-x}Co_xO_{15-\delta}$ as a function of temperature in air. The oxygen content and average oxidation state of 3d-metal ions (z_{Me}) in the $Sm_2Ba_3Fe_{5-x}Co_xO_{15-\delta}$ oxides, either slowly cooled to room temperature or those related to 1100°C (taken from TGA measurements) are listed in Table 1.

Table 1. Oxygen content (15-δ), mean oxidation state of 3*d* metal ions (z_{Me}) ions in $Sm_2Ba_3Fe_{5-x}Co_xO_{15-\delta}$ at 25 and 1100°C together with average thermal expansion coefficients (TECs) calculated from the dilatometry at 1000°C.

Composition	15-δ (25°C) recalculated from [16]	z_{Me} (25°C) [16]	15-δ (1100°C)	z_{Me} (1100°C)	TEC×10^6, K^{-1}
$Sm_2Ba_3Fe_{4.5}Co_{0.5}O_{15-\delta}$	13.80±0.2	3.12	13.40±0.2	2.96	-
$Sm_2Ba_3Fe_4CoO_{15-\delta}$	13.75±0.2	3.10	13.29±0.2	2.92	17.8
$Sm_2Ba_3Fe_{3.5}Co_{1.5}O_{15-\delta}$	13.70±0.2	3.08	13.13±0.2	2.85	17.2

The values of oxygen content and mean oxidation state of 3*d* metal ions (see Fig. 1) are decreasing with the raise of cobalt concentration in $Sm_2Ba_3Fe_{5-x}Co_xO_{15-\delta}$ within the entire temperature range. The amount of oxygen losses while heating from room temperature up to 1100°C ($\Delta\delta = \delta_{1100°C} - \delta_{25°C}$) also gradually increases with Co content. These trends can be explained in terms of binding energy between and 3*d*-metal and oxygen, which is smaller for Co in comparison with Fe ions ($\Delta H°_{Fe-O}$ = 409(13) kJ/mol, $\Delta H°_{Co-O}$ = 368(21) kJ/mol) [19].

Partial substitution of Co for Fe makes decreasing the slope of relative linear expansion versus temperature for $Sm_2Ba_3Fe_{5-x}Co_xO_{15-\delta}$ (x=1; 1.5) compared to Co-free sample (Fig. 2). Excellent reproducibility and absence of hysteresis between the dilatometric data collected on heating and cooling,

indicate high rate of oxygen exchange and confirm absence of phase transition within the temperature range studied. The average thermal expansion coefficients (TECs) calculated from the dilatometry are listed in Table 1.

The temperature dependencies of total conductivity and Seebeck coefficient for $Sm_2Ba_3Fe_{5-x}Co_xO_{15-\delta}$ in air are shown in Figs 3a and 3b. The positive value of Seebeck coefficient (Fig. 3b) indicates predominant *p*-type conductivity in $Sm_2Ba_3Fe_{5-x}Co_xO_{15-\delta}$. Interestingly that conductivity of the sample with x=1 at T>400°C is close to Co-free oxide while the value for $Sm_2Ba_3Fe_{3.5}Co_{1.5}O_{15-\delta}$ is noticeably higher (Fig. 3a). It can be seen in the inset of Fig. 1 that the mean oxidation state of 3*d*-metal is greater than 3 (z_{Me}>3) in $Sm_{1.875}Ba_{3.125}Fe_5O_{15-\delta}$ within entire temperature range, while in Co-doped oxides (x=1.0 and 1.5) its value is much smaller. This means that concentration of mobile holes according to a simple electroneutrality approach should be higher in the Co-free sample.

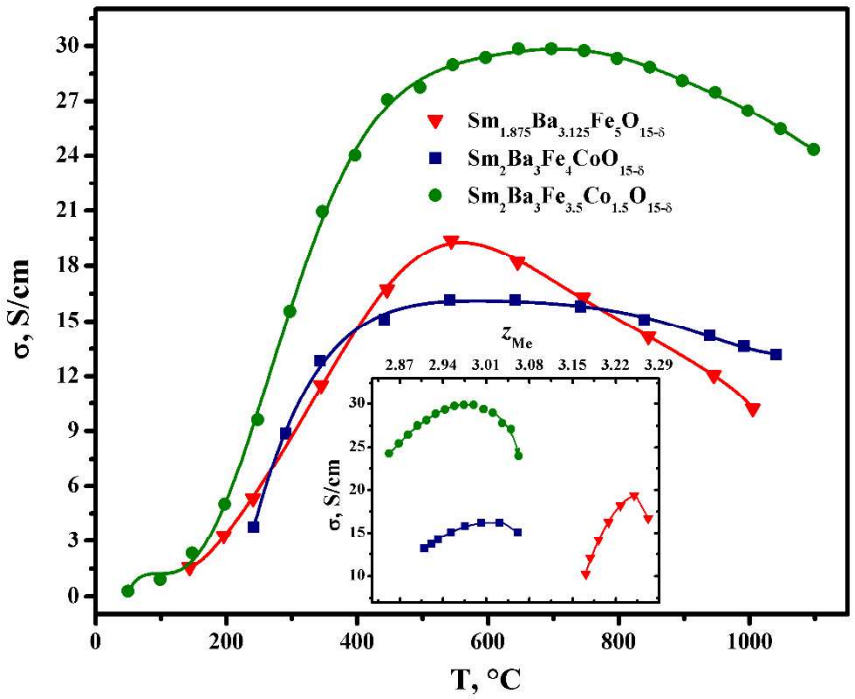
σ, S/cm
T, °C
$Sm_{1.875}Ba_{3.125}Fe_5O_{15-\delta}$
$Sm_2Ba_3Fe_4CoO_{15-\delta}$
$Sm_2Ba_3Fe_{3.5}Co_{1.5}O_{15-\delta}$
z_{Me}
2.87 2.94 3.01 3.08 3.15 3.22 3.29

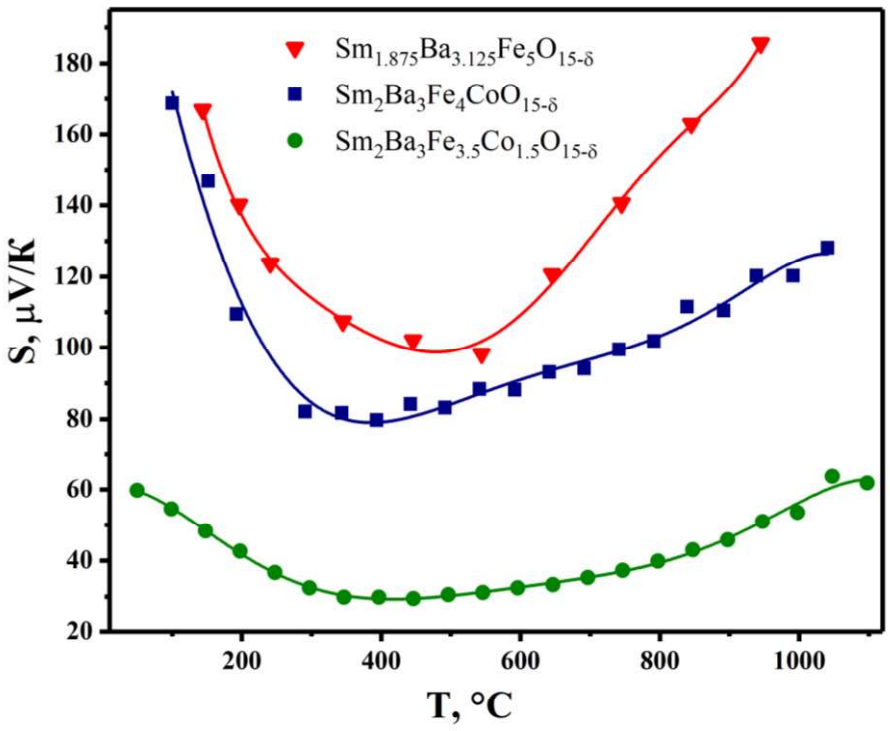
S, μV/K
T, °C
$Sm_{1.875}Ba_{3.125}Fe_5O_{15-\delta}$
$Sm_2Ba_3Fe_4CoO_{15-\delta}$
$Sm_2Ba_3Fe_{3.5}Co_{1.5}O_{15-\delta}$

Moreover, z_{Me}<3 in Co-doped oxides at T>630°C for x=1 and T>530°C for x=1.5, therefore electronic holes can appear only by means of intrinsic charge disproportionation process:

$$2M_{Fe}^{\times} \rightarrow M'_{Fe} + M_{Fe}^{\bullet} \qquad (1)$$

Indeed, such temperature activated disproportionation is well acknowledged in rare earth cobaltites and ferrites with perovskite structure [20-24].

Simultaneous presence of Fe and Co in B-sublattice makes such electronic disordering exchange process even more pronounced:

$$Co_{Fe}^{\times} + Fe_{Fe}^{\times} \rightarrow Co'_{Fe} + Fe_{Fe}^{\bullet} \qquad (2)$$

since Co as more electronegative elements serves as acceptor-type substituent.

Predominant coexistence of Fe^{3+}/Fe^{4+} ions in the studied Co-free oxide and related perovskite materials [25] allow neglected disproportionation of Fe^{3+}. Thus, although on the one hand the raise of Co content makes decreasing oxygen content, and therefore the value of z_{Me} (see inset in Fig. 3a), on the other hand it enhances electronic exchange process (2) and therefore increases charge carrier concentration. This peculiar role of trivalent cobalt is consistent with the sign of the Seebeck coefficient being either positive or negative depending on doping in $LaCoO_3$ [26].

The raise of total conductivity with temperature up to a maximum value at T ≈ 550-750°C can be explained by the increase of mobility and

concentration of electronic holes that appear according to equation (1). At higher temperatures (T>600°C), the total conductivity slightly decreases that caused by an increase in oxygen deficiency, which is preventing formation of electron holes ($M_{Fe}^{\bullet}$) according to the reaction:

$$2Me_{Fe}^{\bullet} + O_O^{\times} \rightarrow 2Me_{Fe}^{\times} + V_O^{\bullet\bullet} + \frac{1}{2}O_2 \qquad (2)$$

Similar temperature dependencies with maximum were obtained for a number of related double perovskite materials [1, 5-7. 9-11].

Conclusion

The $Sm_2Ba_3Fe_{5-x}Co_xO_{15-\delta}$ (x = 0.5, 1.0 and 1.5) oxides have been synthesized by the glycerin nitrate technique in air. Introduction of cobalt decreases the value of oxygen content as well as mean oxidation state of 3*d* metals and allows formation of single-phase 5-fold layered superstructure without Sm/Ba ratio shift comparing to ideal stoichiometric composition (ε=0). This Co-substitution slightly decreases TEC values. Electrical conductivity versus temperature of $Sm_2Ba_3Fe_{5-x}Co_xO_{15-\delta}$ exhibit maxima at relatively high temperature; this is explained by the progressive oxygen losses starting at high temperature. Interestingly, the first step of Co-substitution (x=1.0) has not affected conductivity since two opposite factors, i.e. decrease in oxygen content and enhanced electronic exchange between Fe^{3+} and Co^{3+} ions, compensate each other. Further incorporation of Co (x=1.5) facilitating the latter leads an increase of the conductivity.

Acknowledgement

The work was financially supported in parts from the Ministry of Science and Higher Education of Russian Federation (Agreement No. 075-15-2019-1924) and Russian Foundation for Basic Research (project No 18-33-00822).

References

[1] A.K. Azad, J.H. Kim, J.T.S. Irvine, Structure–property relationship in layered perovskite cathode $LnBa_{0.5}Sr_{0.5}Co_2O_{5+\delta}$ (Ln=Pr,Nd) for solid oxide fuel cells, J. Power Sources 196 (2011) 7333–7337. doi:10.1016/j.jpowsour.2011.02.063.

[2] A. Chang, S.J. Skinner, J.A. Kilner, Electrical properties of $GdBaCo_2O_{5+x}$ for ITSOFC applications, Solid State Ion. 177 (2006) 2009–2011. doi:10.1016/j.ssi.2006.05.047.

[3] M.V. Ananyev, V.A. Eremin, D.S. Tsvetkov, N.M. Porotnikova, A.S. Farlenkov, A.Yu. Zuev, A.V. Fetisov, E.Kh. Kurumchin, Oxygen isotope exchange and diffusion in $LnBaCo_2O_{6-\delta}$ (Ln=Pr,Sm,Gd) with double perovskite structure, Solid State Ion. 304 (2017) 96–106. http://dx.doi.org/10.1016/j.ssi.2017.03.022.

[4] Z. Du, K. Li, H. Zhao, X. Dong, Y. Zhanga, K. Świerczek, A $SmBaCo_2O_{5+\delta}$ double perovskite with epitaxially grown $Sm_{0.2}Ce_{0.8}O_{2-\delta}$ nanoparticles as a promising cathode for solid oxide fuel cells, J. Mater. Chem. A 8 (2020) 14162–14170. http://dx.doi.org/10.1039/d0ta05602b.

[5] D. Chen, F. Wang, H. Shi, R. Ran, Z. Shao, Systematic evaluation of Co-free $LnBaFe_2O_{5+\delta}$ (Ln = Lanthanides or Y) oxides towards the application as cathodes for intermediate-temperature solid oxide fuel cells, Electrochim. Acta 78 (2012) 466–474. https://doi.org/10.1016/j.electacta.2012.06.073.

[6] Z. He, L. Xia, Y. Chen, J. Yu, X. Huang, Y. Yu, Layered perovskite $Sm_{1-x}La_xBaFe_2O_{5+\delta}$ as cobalt-free cathodes for IT-SOFCs, RSC Adv. 5 (2015) 57592–57598. https://doi.org/10.1039/c5ra09762b.

[7] F. Meng, T. Xia, J. Wang, Z. Shi, H. Zhao, Praseodymium-deficiency $Pr_{0.94}BaCo_2O_{6-\delta}$ double perovskite: A promising high performance cathode material for intermediate-temperature solid oxide fuel cells, J. Power Sources 293 (2015) 741-750. http://dx.doi.org/10.1016/j.jpowsour.2015.06.007.

[8] Y.N. Kim, J.H. Kim, A. Manthiram, Effect of Fe substitution on the structure and properties of $LnBaCo_{2-x}Fe_xO_{5+\delta}$ (Ln = Nd and Gd) cathodes, J. Power Sources195 (2010) 6411–6419. https://doi.org/10.1016/j.jpowsour.2010.03.100.

[9] F. Jin, H. Xu, W. Long, Y. Shen, T. He, Characterization and evaluation of double perovskites $LnBaCoFeO_{5+\delta}$ (Ln=Pr and Nd) as intermediate-temperature solid oxide fuel cell cathodes, J. Power Sources 243 (2013) 10-18. http://dx.doi.org/10.1016/j.jpowsour.2013.05.187.

[10] L. Zhao, J. Shen, B. He, F. Chen, C. Xia, Synthesis, characterization and evaluation of $PrBaCo_{2-x}Fe_xO_{5+\delta}$ as cathodes for intermediate-temperature solid oxide fuel cells, Int. J. Hydrogen Energy 36 (2011) 3658–3665. https://doi.org/10.1016/j.ijhydene.2010.12.064.

[11] N.E. Volkova, L.Ya. Gavrilova, V.A. Cherepanov, T.V. Aksenova, V.A. Kolotygin, V.V. Kharton, Synthesis, crystal structure and properties of $SmBaCo_{2-x}Fe_xO_{5+\delta}$, J. Solid State Chem. 204 (2013) 219–223. https://doi.org/10.1016/j.jssc.2013.06.001.

[12] N.E. Volkova, O.I. Lebedev, L.Ya. Gavrilova, S. Turner, N. Gauquelin, Md.M. Seikh, V. Caignaert, V.A. Cherepanov, B. Raveau, G. Van Tendeloo, Nanoscale Ordering in Oxygen Deficient Quintuple Perovskite $Sm_{2-\varepsilon}Ba_{3+\varepsilon}Fe_5O_{15-\delta}$: Implication for Magnetism and Oxygen Stoichiometry, Chem. Mater. 26 (2014) 6303–6310. https://doi.org/10.1021/cm503276p.

[13] A.K. Kundu, O.I. Lebedev, N.E. Volkova, Md.M. Seikh, V. Caignaert, V.A. Cherepanov, B. Raveau, Quintuple perovskites $Ln_2Ba_3Fe_{5-x}Co_xO_{15-\delta}$ (Ln=Sm,Eu): nanoscale ordering and unconventional magnetism, J. Mater. Chem. C 3 (2015) 5398–5405. https://doi.org/10.1039/C5TC00494B.

[14] A.K. Kundu, M.Yu. Mychinko, V. Caignnaert, O.I. Lebedev, N.E. Volkova, K.M. Deryabina, V.A. Cherepanov, B. Raveau, Coherent intergrowth of

simple cubic and quintuple tetragonal perovskites in the system $Nd_{2-\varepsilon}Ba_{3+\varepsilon}(Fe,Co)_5O_{15-\delta}$, J. Solid State Chem. 231 (2015) 36–41. https://doi.org/10.1016/j.jssc.2015.07.050.

[15] N.E. Volkova, A.S. Urusova, L.Ya. Gavrilova, A.V. Bryuzgina, K.M. Deryabina, M.Yu. Mychinko, O.I. Lebedev, B. Raveau, V.A. Cherepanov, Specific Features of Phase Equilibriums in Ln–Ba–Fe–O Systems, Russ. J. Gen. Chem 86 (2016) 1800-1804. https://doi.org/10.1134/S1070363216080041.

[16] N.E. Volkova, M.Yu. Mychinko, I.B. Golovachev, A.E. Makarova, M.V. Bazueva, E.I. Zyaikin, L.Ya. Gavrilova, V.A. Cherepanov, Structure and properties of layered perovskites $Ba_{1-x}Ln_xFe_{1-y}Co_yO_{3-\delta}$ (Ln = Pr, Sm, Gd), J. Alloys Compd. 784 (2019) 1297-1302. https://doi.org/10.1016/j.jallcom.2018.12.391.

[17] Q. Zhou, L. Chen, Y. Cheng, Y. Xie, Cobalt-free quintuple perovskite $Sm_{1.875}Ba_{3.125}Fe_5O_{15-\delta}$ as a novel cathode for intermediate temperature solid oxide fuel cells, Ceram. Intern. 42 (2016) 10469–10471. https://doi.org/10.1016/j.ceramint.2016.03.174.

[18] A.Yu. Zuev, A.I. Vylkov, A.N. Petrov, D.S. Tsvetkov, Defect structure and defect-induced expansion of undoped oxygen deficient perovskite $LaCoO_{3-\delta}$, Solid State Ion. 179 (2008) 1876–1879. http://dx.doi.org/10.1016/j.ssi.2008.06.001.

[19] T.L. Cottrell, The Strengths of Chemical Bonds, Butterworth, London, 1958, P. 310.

[20] E. Bucher, W. Sitte, Defect chemical analysis of the electronic conductivity of strontium-substituted lanthanum ferrite, Solid State Ion. 173 (2004) 23-28. https://doi.org/10.1016/j.ssi.2004.07.047.

[21] P.M. Raccach, J.B. Goodenough, A localized-electron collective-electron transition in the system $(La,Sr)CoO_3$, J. Appl. Phys. 39 (1968) 1209-1210. http://dx.doi.org/10.1063/1.1656227.

[22] J. Mizusaki, M. Yoshihiro, S. Yamauchi, K. Fueki, Nonstoichiometry and defect structure of the perovskite-type oxides $La_{1-x}Sr_xFeO_{3-\delta}$, J. Solid State Chem., 58 (1985) 257-266. http://dx.doi.org/10.1016/0022-4596(85)90243-9.

[23] J. Mizusaki, Y. Mima, S. Yamauchi, K. Fueki, H. Tagawa, Nonstoichiometry of the perovskite-type oxide $La_{1-x}Sr_xCoO_{3-\delta}$, J. Solid State Chem. 80 (1989) 102-111. http://dx.doi.org/10.1016/0022-4596(89)90036-4.

[24] M.H.R. Lankhorst, H.J.M. Bouwmeester, Determination of oxygen nonstoichiometry and diffusivity in mixed conducting oxides by oxygen coulometric titration. II. Oxygen nonstoichiometry and defect model for $La_{0.8}Sr_{0.2}CoO_{3-\delta}$, J. Electrochem. Soc. 144 (1997) 1268-1273. http://dx.doi.org/10.1149/1.1837581.

[25] J. Song, S. Zhu, De Ning, H.J.M. Bouwmeester, Defect chemistry and transport properties of perovskite-type oxides $La_{1-x}Ca_xFeO_{3-\delta}$, J. Mater. Chem. A 9 (2021) 974–989. http://dx.doi.org/10.1039/d0ta07508f.

[26] A. Maignan, D. Flahaut, S. Hébert, Sign change of the thermoelectric power in $LaCoO_3$, Eur. Phys. J. B 39 (2004) 145–148. https://doi.org/10.1140/epjb/e2004-00179-8.

Ceramics International

Dear Editor,

Please find enclosed the manuscript by I.B. Golovachev, M.Yu. Mychinko, N.E. Volkova, L.Ya. Gavrilova, B. Raveau, A. Maignan, V.A. Cherepanov entitled "Effect of cobalt content on the properties of quintuple perovskites $Sm_2Ba_3Fe_{5-x}Co_xO_{15-\delta}$" submitted for the Ceramics International.

Present paper contains new data which are presented for the first time and never been sent to any other Journals. The paper includes following new results: 1) the values of oxygen content for the solid solutions and their temperature dependencies 2) thermal expansion coefficients for the ceramic $Sm_2Ba_3Fe_{5-x}Co_xO_{15-\delta}$ solid solutions; 3) temperature dependencies of conductivity and Seebeck coefficients for the ceramic $Sm_2Ba_3Fe_{5-x}Co_xO_{15-\delta}$ solid solutions.

I believe that the results will be of interest to a wide range of readers.

Yours sincerely,

Assistant professor N.E. Volkova

Department of Physical and Inorganic Chemistry
Ural Federal University
Lenin av., 51,
Ekaterinburg, 620000
RUSSIA
Tel. : +7(343)2517927
e-mail: Nadezhda.Volkova@urfu.ru

Figure 1

Click here to access/download;Figure;figure 1.tif

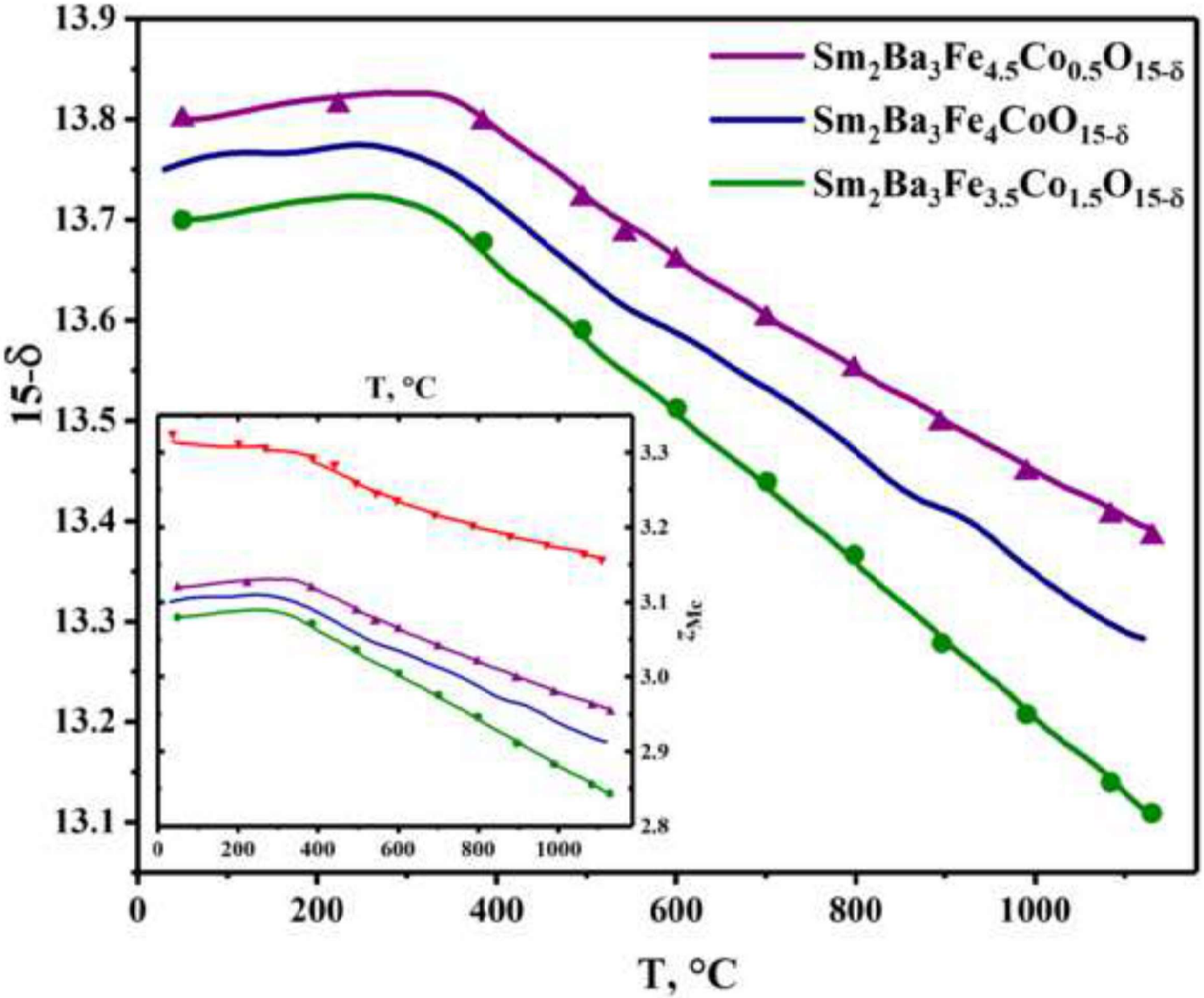

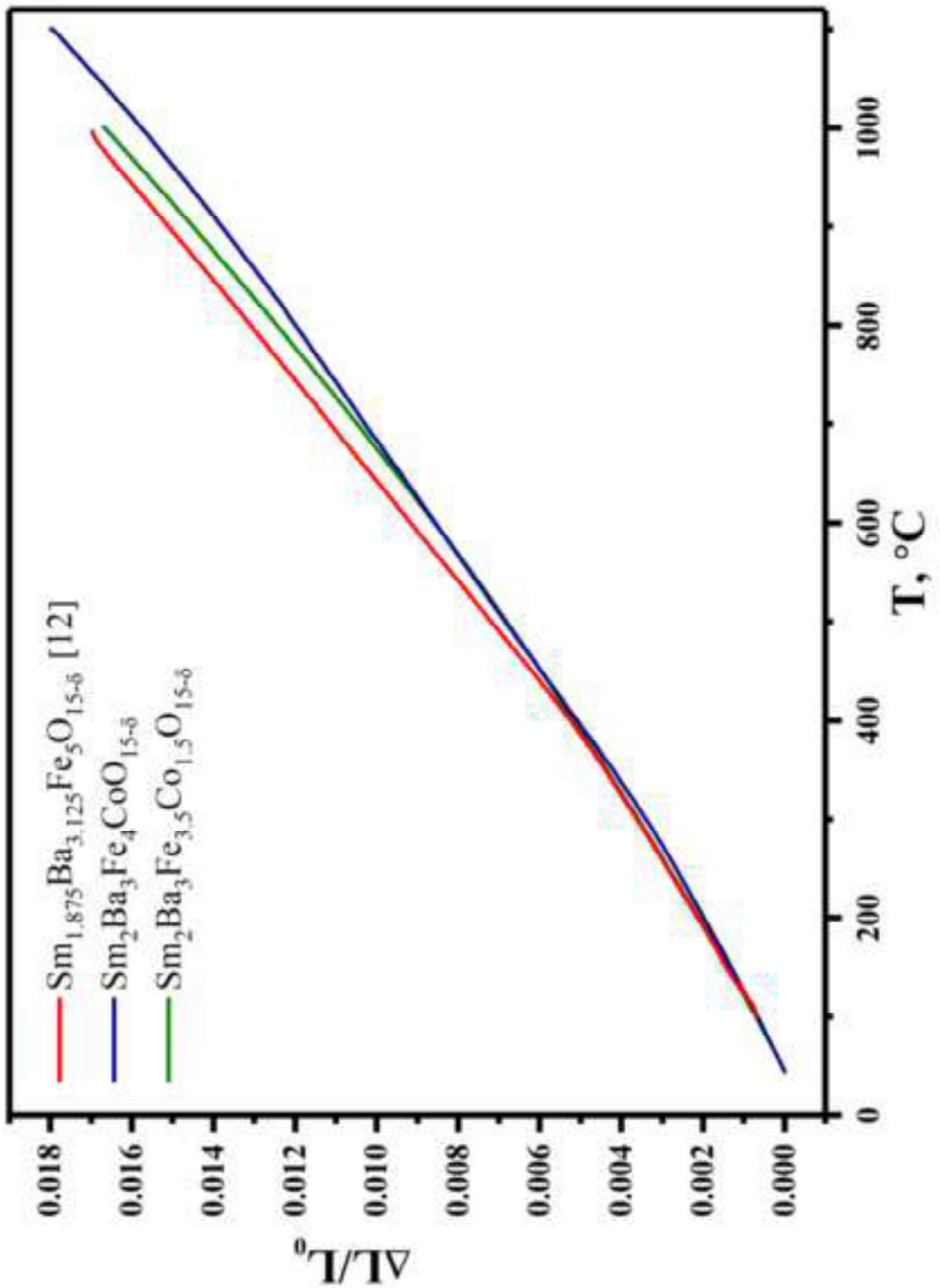

Figure 2

Figure 3a

Click here to access/download;Figure;figure 3a.tif

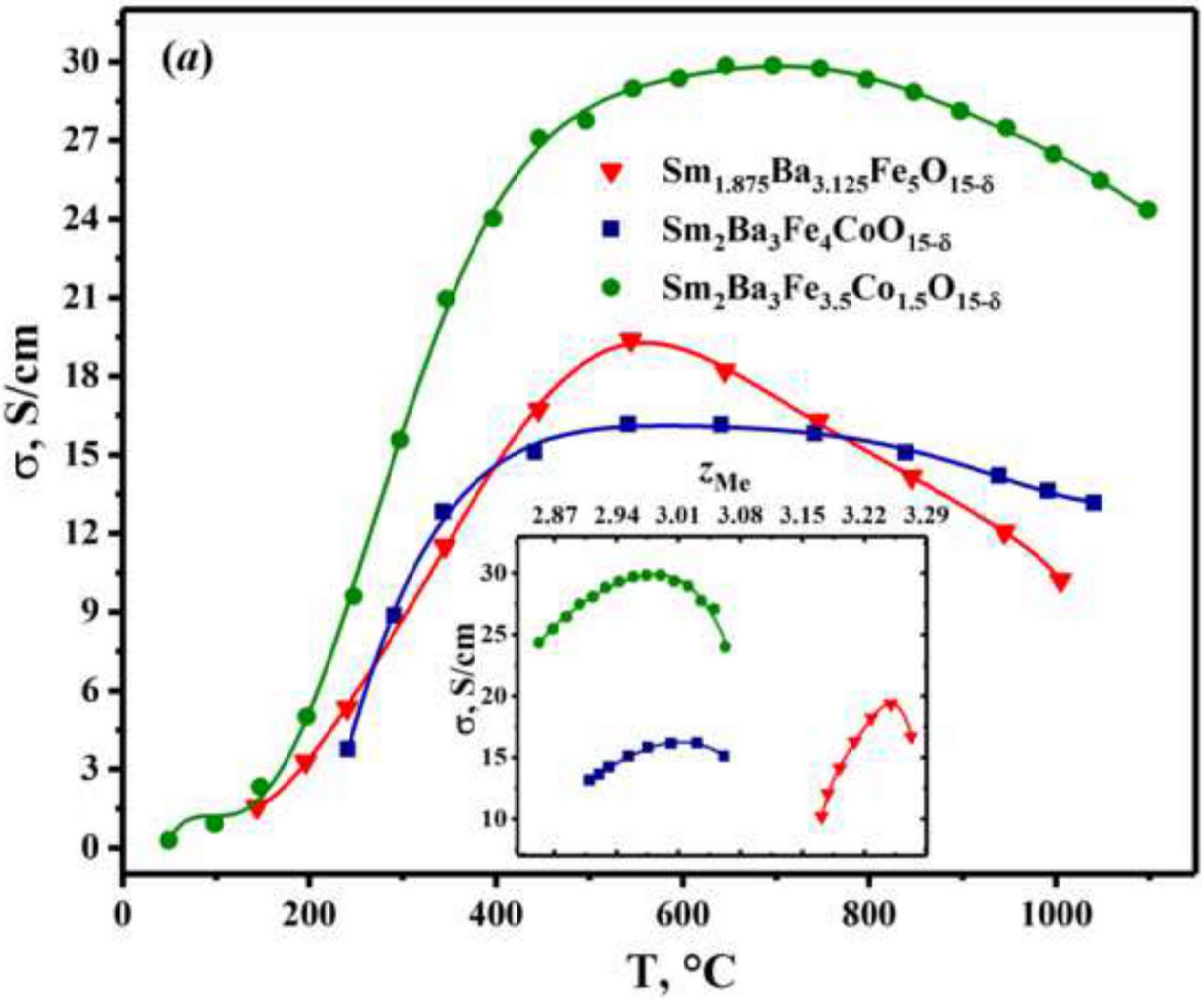

Figure 3b

Click here to access/download;Figure;figure 3b.tif

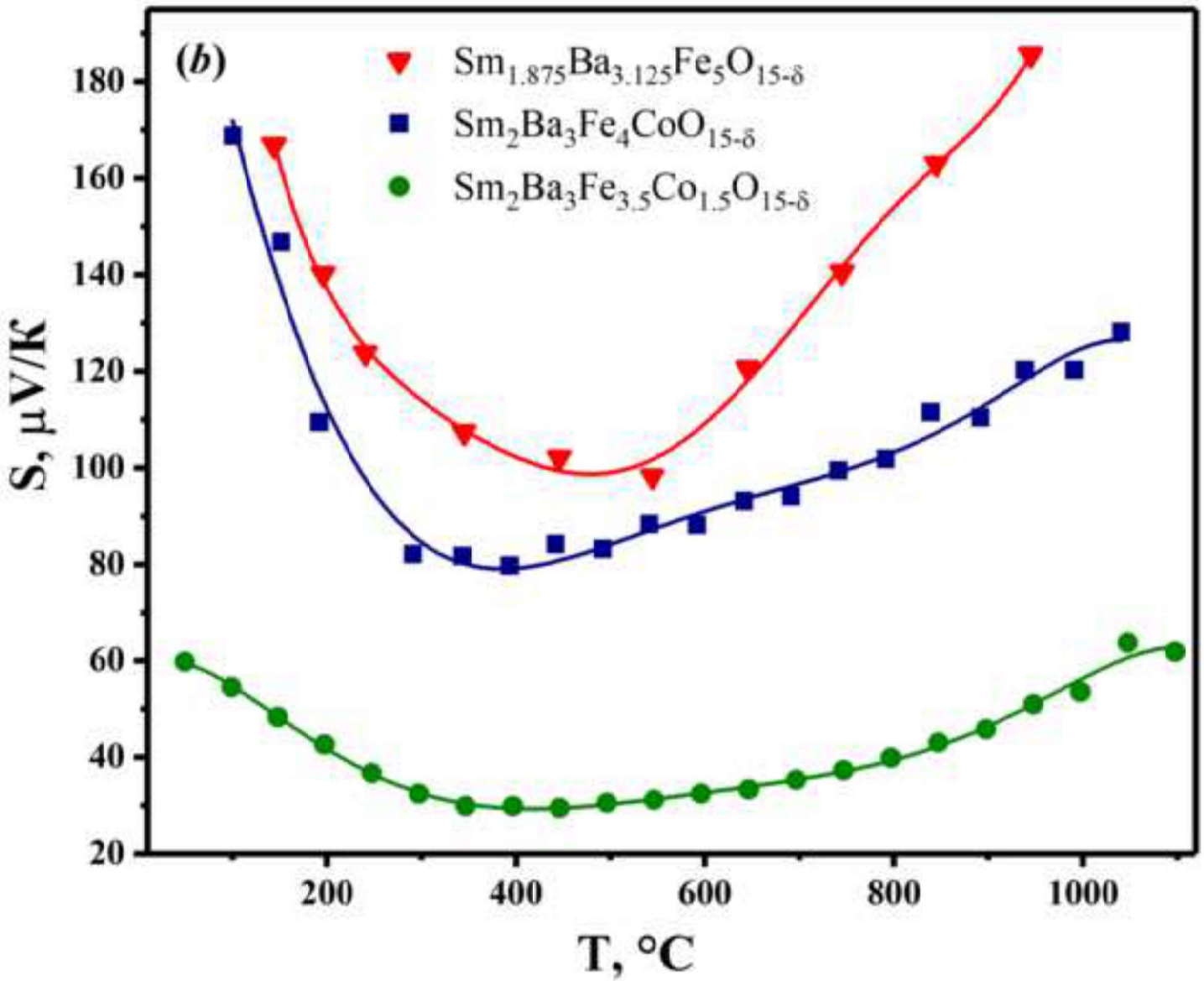

Fig. 1 – Oxygen content in $Sm_2Ba_3Fe_{5-x}Co_xO_{15-\delta}$ at Po_2=0.21 atm. Solid lines represent data obtained in dynamic mode measurements (cooling/heating rate of 5 °C/min), and points correspond to the values measured in static mode (isothermal dwells for 8 h). The inset shows mean oxidation state of 3d metals versus temperature calculated using electroneutrality equation. The plot for Co-free sample (upper red line) was calculated using values of oxygen content presented in [12].

Fig. 2 – Thermal expansion of the $Sm_2Ba_3Fe_{5-x}Co_xO_{15-\delta}$ ceramics in air in comparison with data for $Sm_{1.875}Ba_{3.125}Fe_5O_{15-\delta}$ [12].

Fig. 3 – Temperature dependencies of total conductivity (*a*) and Seebeck coefficient (*b*) for $Sm_{2-\varepsilon}Ba_{3+\varepsilon}Fe_{5-x}Co_xO_{15-\delta}$ in air. Inset in Fig. 3 (a) shows conductivity versus mean oxidation state of 3*d* metals. The values of conductivity for the Co-free sample are taken from [12].

Declaration of interests

☒ The authors declare that they have no known competing financial interests or personal relationships that could have appeared to influence the work reported in this paper.

☐The authors declare the following financial interests/personal relationships which may be considered as potential competing interests:

Supporting Information

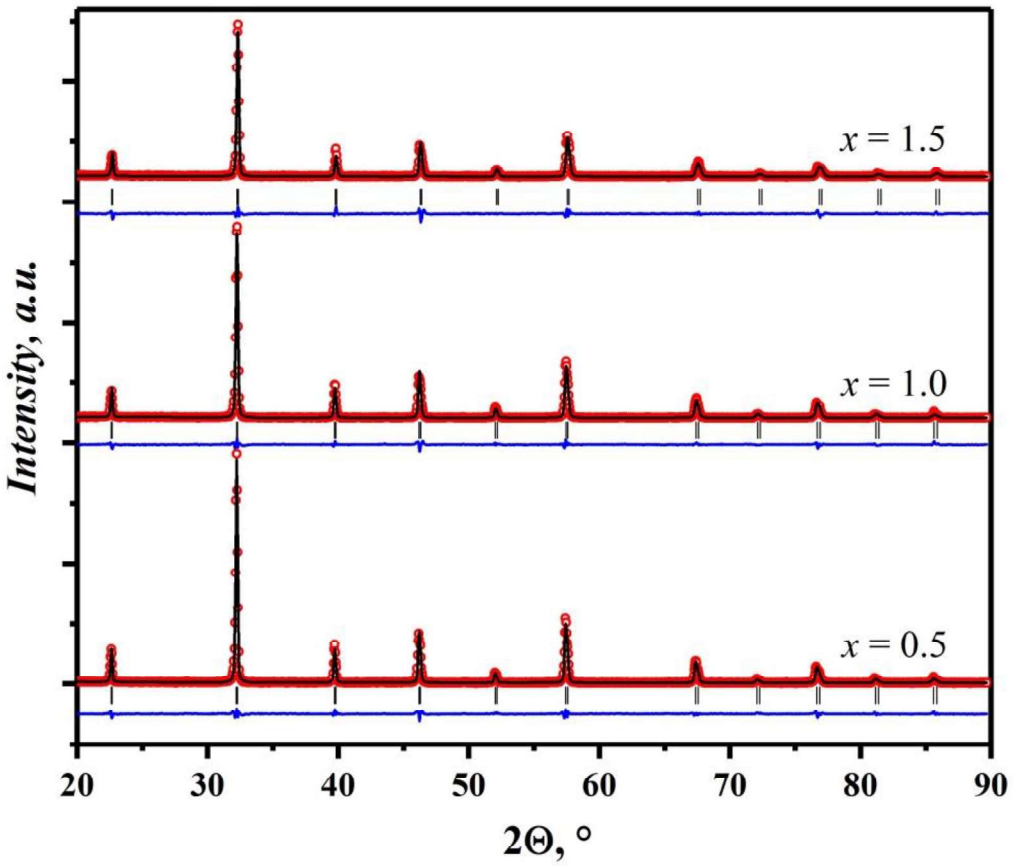

Figure S1. Observed XRD data (points), calculated and difference profiles (solid lines) for the $Sm_2Ba_3Fe_{5-x}Co_xO_{15-\delta}$ samples; vertical lines represent allowed Bragg positions.